JACS
JOURNAL OF THE AMERICAN CHEMICAL SOCIETY

Communication

pubs.acs.org/JACS

Optical Fusion Assay Based on Membrane-Coated Spheres in a 2D Assembly

Chunxiao Bao, Gesa Pähler, Burkhard Geil, and Andreas Janshoff*

Institute of Physical Chemistry, Georg-August-University, Tammannstrasse 6, 37077 Göttingen, Germany

Supporting Information

ABSTRACT: A major goal in neurophysiology and research on enveloped viruses is to understand and control the biology and physics of membrane fusion and its inhibition as a function of lipid and protein composition. This poses an experimental challenge in the realization of fast and reliable assays that allow us, with a minimal use of fluorescent or radioactive labels, to identify the different stages of membrane−membrane interaction ranging from docking to complete membrane merging. Here, an optical two-dimensional fusion assay based on monodisperse membrane-coated microspheres is introduced, allowing unequivocal assignment of docking and membrane fusion. The hard-sphere fluid captures and quantifies relevant stages of membrane fusion and its inhibition without interference from aggregation, liposome rupture, extensive fluorescence labeling, and light scattering. The feasibility of the approach is demonstrated by using an established model system based on coiled-coil heterodimers formed between two opposing membrane-coated microspheres.

Membrane fusion is a fundamental process in life that makes it possible to exchange molecules and material between compartments which otherwise cannot cross membrane barriers.[1] Fusion plays a key role not only in exocytosis of eukaryotic cells but also in viral infection and intracellular fusion of organelles. In this context, the coiled-coil regions of viral matrix proteins such as gp41 of human immunodeficiency virus (HIV) or the influenza surface glycoprotein hemagglutinin (HA) are important targets for drugs to prevent viral fusion.[2] Inhibition of viral fusion by preventing assembling of coiled-coil complexes is a key strategy to abolish viral infection in an early state.[3] Screening assays to find small molecular inhibitors that impede a fusion competent state mainly rely on fluorescence enzyme-linked immunosorbent assays (ELISAs) and specialized cell−cell assays.[4] While ELISAs target the binding affinity between the inhibitor and the coiled-coil structure, cell-based assays directly measure fusion efficiency using tailored effector and reporter cells. Furthermore, vesicle-based fusion assays employing small-molecule recognition, such as complementary DNA strands, or between fusogens bearing vancomycin glycopeptides and D-Ala-D-Ala targets are widely used.[5] However, no assay exists that allows us to directly address docking, hemifusion, and full fusion of cells with virus particles or vesicles in a quantitative and unequivocal manner.

Here, we introduce a robust and versatile fusion assay based on membrane-coated spheres in a 2D assembly that allows optical inspection of membrane−membrane interaction in 96-well plates and highly precise assignment of the various stages of fusion from docking initiated by molecular recognition events to hemifusion up to full membrane merging of both leaflets.[6] The initial idea of the present assay is based on the seminal work of Groves and co-workers, who used the colloidal fluid as a transducer to investigate ligand binding to membrane-coated microspheres.[7] The assay allows the investigation of a large number of interaction partners in a quasi-native environment by automated image analysis on a single-particle basis. Essentially, the strategy relies on two populations of monodisperse silica microspheres, so-called beads, differing visibly in size, which are covered with lipid bilayers obtained from spreading of unilamellar vesicles (Figure 1a) as previously used to investigate binding of cholera toxin.[7a,c] Here, the 2D colloidal hard-sphere fluid makes it possible to monitor the different states of membrane fusion as well as its prevention with externally supplied inhibitors.

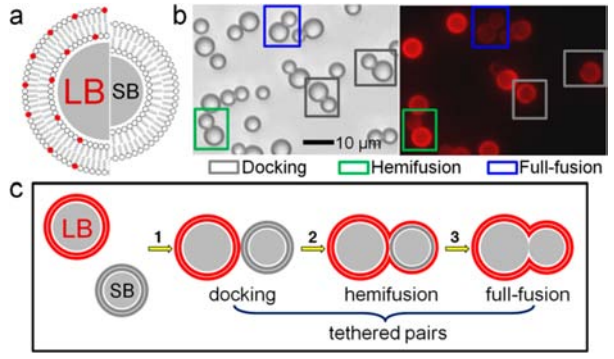

Figure 1. Principle of the 2D fusion assay with membrane-coated beads. (a) Membrane-coated large and small silica beads (LB and SB). Membrane covering LB is fluorescently labeled with Texas Red-DHPE (red). (b) Bright-field (left) and corresponding fluorescence image (right) of LB-*i*-K3 and SB-*i*-E3 on a surface. From the distribution of the fluorescent probe, docked pairs (gray box) and hemifused pairs (green box) as well as fully fused pairs (blue box) can be clearly distinguished. (c) Schematic illustration of conceivable scenarios after mixing of LB and SB: plain docking (1) followed by hemifusion (2) and eventually full fusion of the bilayer (3). All pairs consisting of exactly one LB and one SB, regardless of interaction state of the employed lipid bilayers, are considered as tethered pairs.

Received: April 24, 2013
Published: August 5, 2013

dx.doi.org/10.1021/ja404071z | J. Am. Chem. Soc. 2013, 135, 12176−12179

Even though the membranes on the small beads (SB, diameter 4.7 μm) are not fluorescently labeled, both bead populations can be readily distinguished by size discrimination using an optical microscope (Figure 1b, left). The fluorescence label embedded in the lipid bilayer covering the large beads (LB, diameter 6.5 μm) allows us to detect fusion events by fluorescence microscopy of the same area (Figure 1b, right). This enables us to simultaneously quantify docking, hemifusion, and full fusion.

Typical disadvantages of conventional bulk fusion assays based on liposomes are uncontrolled aggregation of vesicles and light scattering interfering with fluorescence emission.[8] Most approaches require an extensive amount of fluorescence labels to reach a self-quenched state, which therefore might compromise the fusogenic properties of peptides and proteins by altering the zeta potential of the liposomes and changing the microenvironment of the decisive constituents. Giant unilamellar vesicles (GUVs) which would conceivably be attractive replacements for the beads are considerably more polydisperse and display thermally excited membrane undulation, which requires very strong attractive forces to overcome the barrier posed by this so-called Helfrich repulsion. Moreover, two GUVs merge into a single, larger vesicle, preventing the ability to reconstruct the history with only one label. This is because GUVs display large size differences and are hardly visible in conventional microscopy without labels. Also often ignored are the inevitable osmotic gradients between the interior of the liposome and the external solution. Considering that area dilatation of lipid bilayers is limited to only few percent, a change in osmolarity of 5−10 mM is sufficient to rupture the GUVs in a size regime of 50−100 μm, not to mention that stress fosters fusion.

The use of monodisperse silica beads as a support for the lipid bilayer solves problems associated with membrane tension, undulations, and most importantly excessive labeling. However, the solid support also poses limitations to the usability of this assay. Obviously, content mixing is not possible in our case, which narrows the use in cargo-delivering applications. Also the support restricts membrane composition as the bilayer is formed from vesicles spreading on the curved substrate. The fraction of negatively charged phospholipids such as PI, PS, or PG is limited to around 20%. Whether the advantages outweigh the disadvantages originating from the solid support depends on the scientific question. Since we are not interested in delivering cargo, beads are advantageous in identifying inhibitors of fusion. The envisioned read-out of membrane fusion is illustrated in Figure 1c, corresponding to what is shown experimentally in Figure 1b. Starting with two bead populations differing in size and composition of the lipid membranes, all connected bead pairs consisting of exactly one LB and one SB after a specific incubation time of 90 min are considered and are called tethered pairs in the following. From these tethered pairs, the three main steps of membrane fusion, i.e., docking, hemifusion, and full fusion, can be easily distinguished by reading out the fluorescence intensity of the lipid membranes covering connected LB and SB pairs, while simultaneously taken bright-field microscopy images allow the detection of all beads. A fluorescent membrane on a LB in contact with a dark SB characterizes docking without fusion. In this Communication, the term "hemifusion" is used synonymously with merging of the two outer membrane leaflets. Therefore, this term is not thoroughly precise since the molecular organization concerning incipient stalk formation and a fully formed diaphragm-shaped hemifusion in the contact area is yet unknown.[9]

For proof of concept, we used the well-established fusogenic E-peptides (*i*-E3Cys) and K-peptides (*i*-K3Cys) coupled to a lipid anchor MCC-DOPE embedded in the deposited bilayer.[10] These peptides are known to form heterodimeric coiled-coil structures, which initiate docking between two lipid bilayers and eventually facilitate membrane fusion.[11] LBs were coated with a lipid bilayer composed of DOPC/MCC-DOPE/Texas Red-DHPE (89.5:10:0.5, all given in mol%), while SBs were decorated with a DOPC/MCC-DOPE (90:10) bilayer. The maleimide-bearing lipid MCC-DOPE allows a covalent coupling of fusogenic peptides to the membrane surface to demonstrate the feasibility of this assay (Figure S1). Coupling efficiency of peptides to the maleimide headgroup is around 50−75%, as demonstrated by ellipsometry measurements (Figures S2 and S3).[12] We found that regardless of the helix orientation, coiled-coil dimers anchored to a lipid bilayer display K_D values in the micromolar regime ($K_D \approx 25$ μM).[11b] Concerted binding of many complementary peptides, however, produces a very large free binding energy, making it possible to overcome the fusion barrier (Figure 2a).

The two populations of beads are mixed and then deposited in a 96-well plates, forming a mobile 2D hard-sphere fluid. The

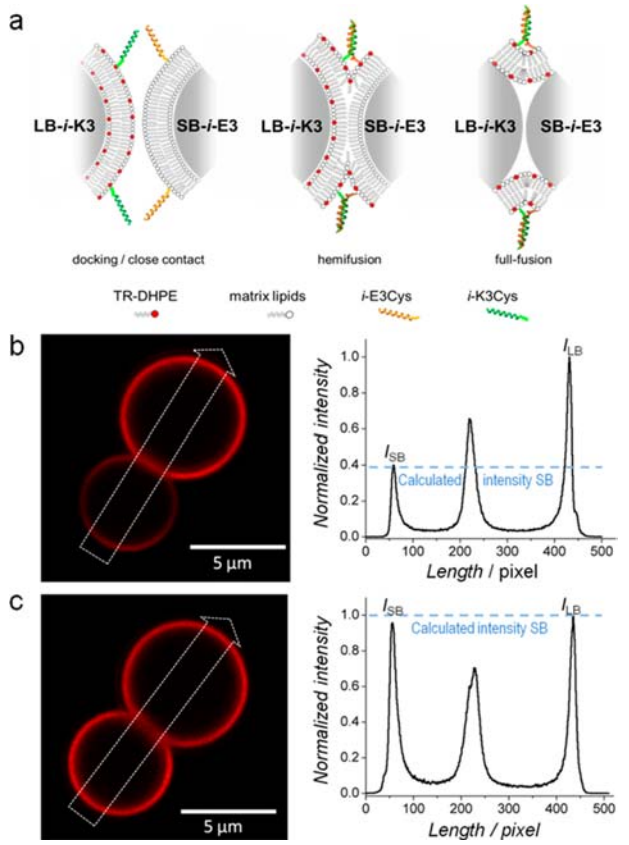

Figure 2. Classification and proof of principle considering membrane−membrane interaction triggered by coiled-coil formation between LBs and SBs. (a) Illustration of approach/docking (left), hemifusion (center), and full fusion (right) of membrane-coated beads (LB-*i*-K3/SB-*i*-E3) by formation of parallel coiled-coil peptide dimers. (b,c) Intensity analysis using a broad line profile (white arrow) across a pair consisting of LB-*i*-K3/SB-*i*-E3 imaged with a confocal laser scanning microscope. Peaks correspond to relative fluorescence intensity of SB, merged area, and LB. Scattered line shows calculated I_{SB}. Hemifusion is shown in (b) with an intensity ratio between LB:SB of 1:0.4 as expected (see SI), while (c) shows full fusion of both leaflets (LB:SB 1:0.95).

dx.doi.org/10.1021/ja404071z | *J. Am. Chem. Soc.* 2013, 135, 12176−12179

beads display Brownian motion on the surface (Figure S4), which allows them to self-assemble according to their interparticle affinity.[7c] Bright-field images (Figure 1b, left) allow counting of all bead pairs (tethered pairs).

From the corresponding fluorescence micrograph, the fluorescence intensity of the membrane on the LB-*i*-K3 and SB-*i*-E3 is obtained. If the two beads are only docked without exchange of lipid material, no fluorescence intensity is observed on the SB-*i*-E3 (gray box in Figure 1b). If, however, hemifusion occurred, a fluorescently labeled membrane becomes discernible on the SB-*i*-E3 (green box in Figure 1b). Full fusion could be achieved if additionally Ca^{2+} ions were added, as was recently found to lead to content mixing in vesicle assays.[11b]

Unequivocal identification of docking, hemifusion, and full fusion was accomplished by intensity analysis across the corresponding LB/SB pair (Figure 2b,c). We assign pairs with a fluorescence intensity ratio of 1:0.4 (LB:SB) to hemifusion (Figure 2b and SI), while an intensity ratio of 1:1 was attributed to full fusion (Figure 2c). Interestingly, we find a reduced intensity in the contact zone of the fully fused pairs, which is due to lipid depletion in the contact area (*vide infra*).

Ultimate proof that a continuous membrane has been formed after docking of two beads is provided by fluorescence recovery after photobleaching (FRAP) experiments (Figure 3). Moreover, the experiment also allows us to estimate the size of the contact zone by comparing the data to simulations assuming the same geometry. Figure 3a shows FRAP data acquired on a single LB, showing membrane fluidity as expected ($D \approx 1\ \mu m^2/s$) for solid supported lipid bilayers.[13] After fully bleaching the fluorophors on the SB-*i*-E3 that is in contact to a LB-*i*-K3 either hemifused or fully fused (Figure 3b,c), the intensity recovery is slowed down by more than 2 orders of magnitude compared to the diffusion from geometrically unrestricted membranes (Figure 3a), which is attributed to the small contact zone between the beads forming a bottleneck for lipid diffusion. This experimental finding is supported by Monte Carlo simulations assuming identical geometry and initial conditions such as a fixed diffusion constant (Figure 3c and SI). By assuming a contact angle of 10° corresponding to a contact radius of $a_{FRAP} \approx 1000$ nm, we could largely reproduce our experimental findings, i.e., the spread in time scales, assuming an unaltered lipid diffusion constant. Interestingly, compared with the contact radius predicted by Hertzian contact mechanics ($a_{Hertz} \approx 35$ nm), we observe a significant larger contact zone after hemifusion or full fusion (see SI). The time delay between FRAP of single beads and dimers of beads can therefore be mapped directly to the contact area formed between the two beads.

Notably, we found almost the same contact zone size for either hemifused or fully fused pairs. It is also important to mention that changing the contact angle from 0° to 90° (cylinder geometry) does not exceed the area dilatation beyond 5%, which is uncritical for bilayer integrity.

Efficiencies concerning docking, hemifusion, and full fusion after incubating the two bead populations for 90 min at different conditions (presence of Ca^{2+} ions and inhibitor *i*-E3Cys) are shown in Figure 4. This is achieved by comparing all docked LB-*i*-K3/SB-*i*-E3 pairs ($N_{docking}$) to hemifused pairs ($N_{hemifusion}$) and fully fused pairs ($N_{full\ fusion}$), respectively. We define $N_{tethering}$ as $N_{tethering} = N_{docking} + N_{hemifusion} + N_{full\ fusion}$. We can calculate the docking efficiency $N_{docking}/N_{tethering}$, hemifusion efficiency $N_{hemifusion}/N_{tethering}$, and the full fusion efficiency $N_{full\ fusion}/N_{tethering}$. Figure 4 clearly shows that the hemifusion efficiency provided high values around 99%, implying that docking within

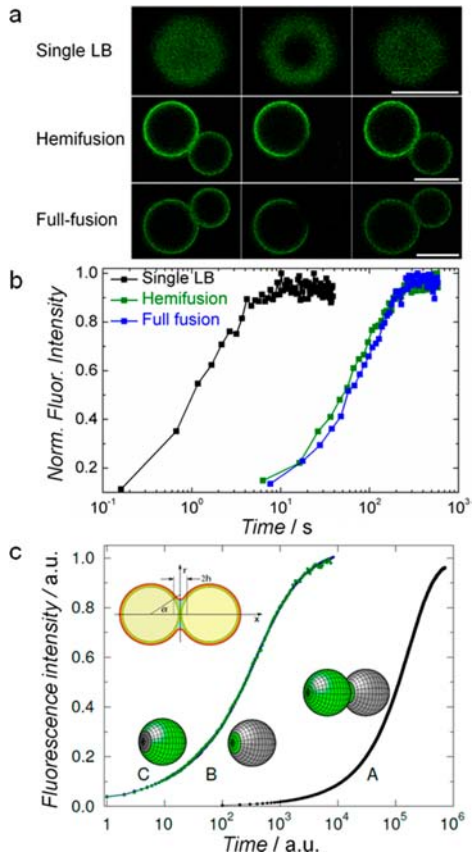

Figure 3. Fluorescence recovery after photobleaching (FRAP) experiments/simulations proving membrane connection between LB-*i*-K3/SB-*i*-E3 through a small contact zone. (a) Fluorescence micrographs prior to bleaching the NBD dyes, directly after bleaching and after fluorescence recovery (from left to right) of a single bead (top), a hemifused pair (center), and a fully fused pair (bottom). The scale bar is 5 μm. (b) FRAP experiment of LB-*i*-K3/SB-*i*-E3 pairs after bleaching the entire SB-*i*-E3 (blue/green) compared to a reference experiment showing fluorescence recovery of a single LB after bleaching a spot on the bead (black). The green curve corresponds to the hemifused pair, while the blue graph represents data from the fully fused one. (c) Monte Carlo simulations of FRAP on a single bead (curves B/C) serving as a reference and dimers sharing one continuous membrane (curve A).

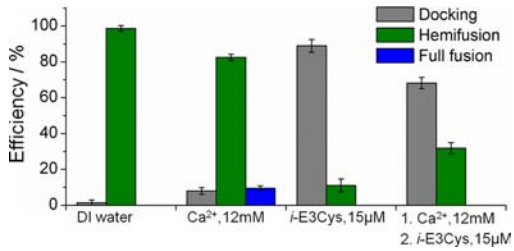

Figure 4. Efficiency of docking (gray), hemifusion (green), and full fusion (blue) of LB-*i*-K3/SB-*i*-E3 pairs as a function of the presence or absence of Ca^{2+} administration to trigger full fusion and presence of externally added inhibitor (*i*-E3Cys). Control experiments with membrane-coated beads in the absence of peptides attached to the membrane shell do not show fusion events and rarely show docking (beyond statistically formed pairs).

the time frame of our experiments leads predominantly to hemifusion. Only after administration of calcium ions we also observe full fusion in good accordance with a previous study employing liposome assays. In this previous study we only

dx.doi.org/10.1021/ja404071z | J. Am. Chem. Soc. 2013, 135, 12176−12179

observed fusion induced by E- and K-peptides in parallel orientation and in the presence of calcium ions.[11b] Even in this case we only record 3% fusion efficiency, which is essentially similar to what we found in this bead assay (8−10%, Figure 4). This implies that bead pairs as well as liposomes are mainly arrested in the hemifused state.

In liposome assays, fusion is driven by the gain in bending energy released by annihilation of one spherical bilayer structure if two liposomes form one larger one ($\sim 400 k_B T$). In our bead assay this energy gain is inherently missing. However, the gain in energy comes from the van der Waals attraction between the two silica beads that come into close contact after fusion, removing all the water in between the two beads.

Using *i*-E3Cys peptides as a competitive inhibitor for the *i*-K3Cys displayed on LB ($c_{i\text{-E3Cys}} = 15\ \mu M$ added to the suspension of beads), we found that (hemi)fusion efficiency was significantly decreased. In the presence of Ca^{2+}, the inhibition was less efficient. The K_D value as determined by ellipsometry measurements is about 25 μM.[11b] However, fusion is inhibited already at lower inhibitor concentrations, probably because of limited lateral mobility after dimer formations. We attribute the association of beads to multivalency effects boosting the association constant of two beads attracting each other and nonspecific electrostatic interactions originating from the peptides themselves.[14] The data show that indeed the assay allows classification and quantification of fusion inhibitors, thereby emphasizing its feasibility for high-throughput and high-content screening of potent viral fusion inhibitors.

In conclusion, we establish a membrane fusion assay that generally allows us to identify the different stages of the fusion process in an ensemble measurement. Membrane fusion driven by heterodimeric coiled-coil formation as a proof of concept using fusogenic K- and E-peptides provided results comparable to those obtained with conventional liposome assays, but with additional information on docking efficiency.[11b] Fusion plays a key role not only in viral infection of particularly enveloped species but also in exocytosis of eukaryotic cells, intracellular fusion of organelles, and the action of fusogenic peptides. Regardless of the biological function, the elementary process of fusion usually comprises membrane contact, partial membrane merger, and eventually formation of a growing aqueous pore indicating complete merging of both leaflets. According to the stalk hypothesis, bilayer fusion proceeds through merging of the outer leaflets, forming a stalk and thereby creating a hemifusion intermediate. Essentially the bilayer system is destabilized by running through non-bilayer states that culminate in the formation of an aqueous pore. In order to study this highly complex process, a number of fusion assays based on artificial model systems mainly involving liposomes have been devised that allow to monitor fusion as function of external parameters comprising lipid and protein composition. So far, no bulk assay has been conceived of that distinguishes among docking, hemifusion, and full fusion without interference from light scattering and use of a single fluorophore at low concentration. By using microspheres, the curvature of fusogenic membranes can be easily controlled and through variation of the employed bead sizes, differences in fusogenity can be addressed. Another problem with conventional assays are the fluorophors embedded in the bilayers. High concentrations needed for dequenching experiments might generate enormous net charges at the vesicle surface that in the presence of divalent ions can lead to unwanted fusion and thereby obscure the effect of dedicated fusion peptides.[15] Moreover, bulk fusion assays carried out in solution are not suitable for high-throughput monitoring of fusion. Our assay, however, can be realized with ordinary laboratory equipment and a minimum of fluorophors, is not hampered by light scattering, and is compliant with high-throughput multi-well techniques. Therefore, we expect our approach to be of general use for determining fusogenity of peptides and an invaluable tool to identify small-molecule inhibitors of viral fusion with unprecedented accuracy.

■ ASSOCIATED CONTENT

Ⓢ Supporting Information

Experimental and calculation details, simulations, and additional characterization data. This material is available free of charge via the Internet at http://pubs.acs.org.

■ AUTHOR INFORMATION

Corresponding Author

ajansho@gwdg.de

Notes

The authors declare no competing financial interest.

■ ACKNOWLEDGMENTS

This work was funded by the German Science Foundation (A.J., project B8 in CRC 803) and the Chinese Government by awarding a China Scholarship Council Fellowship (C.B.).

■ REFERENCES

(1) Jahn, R.; Lang, T.; Südhof, T. C. *Cell* **2003**, *112*, 519.

(2) Chan, D. C.; Chutkowski, C. T.; Kim, P. S. *Proc. Natl. Acad. Sci. U.S.A.* **1998**, *95*, 15613.

(3) Frey, G.; Rits-Volloch, S.; Zhang, X. Q.; Schooley, R. T.; Chen, B.; Harrison, S. C. *Proc. Natl. Acad. Sci. U.S.A.* **2006**, *103*, 13938.

(4) (a) Gochin, M.; Savage, R.; Hinckley, S.; Cai, L. *Biol. Chem.* **2006**, *387*, 477. (b) Ji, C.; Zhang, J.; Cammack, N.; Sankuratri, S. *J. Biomol. Screen.* **2006**, *11*, 65.

(5) (a) Gong, Y.; Luo, Y.; Bong, D. *J. Am. Chem. Soc.* **2006**, *128*, 14430. (b) Ma, M.; Gong, Y.; Bong, D. *J. Am. Chem. Soc.* **2009**, *131*, 16919. (c) Chan, Y.-H. M.; Lenz, P.; Boxer, S. G. *Proc. Natl. Acad. Sci. U.S.A.* **2007**, *104*, 18913. (d) Chan, Y.-H. M.; Van Lengerich, B.; Boxer, S. G. *Proc. Natl. Acad. Sci. U.S.A.* **2009**, *106*, 979.

(6) Tamm, L. K.; Crane, J.; Kiessling, V. *Curr. Opin. Struct. Biol.* **2003**, *13*, 453.

(7) (a) Baksh, M. M.; Jaros, M.; Groves, J. T. *Nature* **2004**, *427*, 139. (b) Bayerl, T. M. *Nature* **2004**, *427*, 105. (c) Winter, E. M.; Groves, J. T. *Anal. Chem.* **2006**, *78*, 174.

(8) (a) Düzgünes, N.; Allen, T. M.; Fedor, J.; Papahadjopoulos, D. *Biochemistry* **1987**, *26*, 8435. (b) Düzgünes, N. *Methods in Enzymology*; Academic Press: San Diego, 2003; Vol. *372*, p 260.

(9) Chernomordik, L. V.; Kozlov, M. M. *Nat. Struct. Mol. Biol.* **2008**, *15*, 675.

(10) Litowski, J. R.; Hodges, R. S. *J. Biol. Chem.* **2002**, *277*, 37272.

(11) (a) Marsden, H. R.; Elbers, N. A.; Bomans, P. H. H.; Sommerdijk, N. A. J. M.; Kros, A. *Angew. Chem., Int. Ed.* **2009**, *48*, 2330. (b) Pähler, G.; Panse, C.; Diederichsen, U.; Janshoff, A. *Biophys. J.* **2012**, *103*, 2295.

(12) Faiss, S.; Schuy, S.; Weiskopf, D.; Steinem, C.; Janshoff, A. *J. Phys. Chem. B* **2007**, *111*, 13979.

(13) (a) Tamm, L. K.; McConnell, H. M. *Biophys. J.* **1985**, *47*, 105. (b) Seu, K. J.; Pandey, A. P.; Haque, F.; Proctor, E. A.; Ribbe, A. E.; Hovis, J. S. *Biophys. J.* **2007**, *92*, 2445.

(14) Gomez, E. W.; Clack, N. G.; Wu, H.-J.; Groves, J. T. *Soft Matter* **2009**, *5*, 1931.

(15) (a) Lee, A. G. *Biochim. Biophys. Acta—Biomembranes* **2004**, *1666*, 62. (b) Repáková, J.; Holopainen, J. M.; Karttunen, M.; Vattulainen, I. *J. Phys. Chem. B* **2006**, *110*, 15403.